ELSEVIER

Materials Science and Engineering A190 (1995) 55-64

MATERIALS SCIENCE & ENGINEERING A

Effects of microstructural variables on the deformation behaviour of dual-phase steel

Zhonghao Jiang[a], Zhenzhong Guan[a], Jianshe Lian[b]

[a] *Changchun Institute of Optics and Fine Mechanics, Chinese Academy of Sciences, Changchun, 130025, China*

[b] *Department of Metal Materials Engineering, Jilin University of Technology, Changchun, 130025, China*

Received 28 July 1993; in revised form 11 April 1994

Abstract

An expression for the stress of martensite in dual-phase steel was developed, which shows the interdependence of the stress of martensite and strain hardening in the ferrite matrix and the contribution of microstructural variables (the volume fraction of martensite f_m, ferrite grain size d_f, and martensite particle size d_m). The onset of plastic deformation of martensite in dual-phase steel was predicted to depend on its yield strength and the microstructural variables, and this was verified by the modified Crussard-Jaoul analysis. It was found that for this dual-phase steel, refining the grain size and increasing f_m increase the flow stress and raise the strain hardening rate at low strains, but little affect the strain hardening rate at high strains. The effect of the ferrite grain size on the flow stress of this dual-phase steel was found to obey the Hall-Petch relation, i.e. $\sigma = \sigma_0^e + K^e d_f^{-1/2}$, where the Hall-Petch intersection σ_0^e and slope K^e are functions of strain, f_m and d_m. The effects of the plastic deformation of martensite and the microstructural variables on the strain hardening rate and the Hall-Petch behaviour were analysed in terms of the densities of statistically stored dislocations and geometrically necessary dislocations using the previously developed theoretical model.

Keywords: Deformation; Steel

1. Introduction

Dual-phase steels are a type of low-carbon low-alloy steel characterized by a microstructure consisting of a ferrite matrix with particles of martensite, and have received considerable attention owing to their superior combination of high strength and good ductility.

A number of attempts have been made to describe the deformation behaviour and structure-properties relationship of dual-phase steels. The classical law of mixture with the assumption of either isostress or isostrain has been used for dual-phase steels [1-4] to predict the tensile properties. A modified form of the law of mixture or intermediate law of mixture was proposed by Tamura et al. [5] and Fischmeister and Karlsson [6], which assumes that the tensile deformation behaviour lies between the states of isostress and isostrain. This model has been used for dual-phase steels by several investigators [7-11] to elucidate the effects of the retained austenite and initial accommodation dislocations [8, 9] and the deformation state of martensite [11].

Tomata et al. [12] proposed a continuum mechanics model in which the internal back stress produced by the inhomogeneous distribution of plastic deformation between two constituents is taken into account. Kim [13] extended the application of this model to dual-phase steel and explained well the effect of strain-induced transformation of retained austenite to martensite. Micromechanics theories, which are based on the dispersion hardening models, such as those of Ashby [14-16] and Brown and Stobbs [17], were developed for dual-phase steel by several authors [18-22]. They explained the effects of grain sizes [18-20], dislocation density [18-22] and the contribution of back stress [19, 21, 22].

In spite of the considerable successes in understanding the deformation behaviour and structure-properties relationships of dual-phase steels, some problems still require further study. For example, the deformation behaviour of the martensite phase is not fully understood. In addition, the Hall-Petch behaviour in dual-phase steel has not been given enough attention.

SSDI 0921-5093(94)09594-M

Recently, a theoretical model [23] for the relationship between the flow stress and the microstructural variables (d_m, d_f and f_m) was proposed based on the Ashby strain hardening theory [15, 16] and the dislocation pile-up concepts. In the present study, this model was used to investigate the effects of the microstructural variables (f_m, d_f and d_m) and the behaviour of martensite on the deformation behaviour of dual-phase steel. Special attention was paid to the Hall–Petch behaviour of dual-phase steel.

2. Experimental procedure

The material used in the present study was a hot rolled steel bar, 14 mm in diameter. The composition of this steel was 0.12 wt.% C, 0.87 wt.% Mn, 0.25 wt.% Si, 0.01 wt.% P, 0.06 wt.% S, 0.08 wt.% V and 0.02 wt.% Al. The steel was first heated at 1100 °C for 4 h and air cooled to obtain a uniform, initial microstructure of ferrite–pearlite. In order to obtain dual-phase steels with different grain sizes, the steel was repeatedly heated to temperatures ranging from 830 to 1000 °C for 1 h followed by furnace cooling. A similar heat treatment method was previously used by Tanaka et al. [24].

Cylindrical tensile specimens with 5 mm gauge diameter and 25 mm gauge length were machined from the treated hars. The dual-phase microstructure was obtained by heating the specimens in a salt bath in the intercritical region for 15 min and quenching in 15% brine to room temperature. The intercritical annealing temperatures were chosen to produce the required volume fractions of martensite. After the above treatments, the specimens were surface ground to final size. The tensile tests were carried out with a cross-head speed of 1 mm min^{-1}. Microstructures of the steel were examined using materials taken from the grip sections of broken tensile test pieces. The volume fractions of martensite were determined using a Quantimet-970 image analyser. The ferrite grain size and martensite particle size were measured manually by the linear intercept method on specimens etched with 3% Nital. The definitions of ferrite grain size and martensite particle size in this study were the same as in a previous study [23].

3. Experimental results

Intercritical annealing at different temperatures followed by rapid quenching produced a polygonal ferrite–martensite structure in all the specimens. At the same intercritical annealing temperature, the ferrite grain size and martensite particle size decreased with decreasing heating temperature and increasing times of pretreatment. The volume fraction of martensite increased with increasing intercritical annealing temperature and was not affected systematically by the pretreatment. Quantitative metallographic results for these dual-phase steels are shown in Table 1, and representative microstructures with varying grain sizes are shown in Fig. 1. The part experimental true stress–strain curves of this dual-phase steel are shown in Fig. 2. The tensile data, the true tensile strength σ_u, the true yield strength $\sigma_{0.2}$ and the maximum uniform true strain ε_u are shown in Table 1. It can be seen that at approximately constant f_m, σ_u and $\sigma_{0.2}$ increase with decreasing grain size and under the same pretreatment conditions, σ_u and $\sigma_{0.2}$ increase with increasing f_m. ε_u decreases with increasing f_m and tends to increase with decreasing grain size.

The dependence of the flow stress on the grain size of this dual-phase steel was examined by plotting the flow stresses at several selected strains against the inverse square root of ferrite grain size $d_f^{-1/2}$, shown in Fig. 3. The flow stress at a given strain increases linearly with $d_f^{-1/2}$, that is, the Hall–Petch relationship holds between the flow stress and ferrite grain size. It is apparent that the Hall–Petch parameters, the intersection σ_0^e and the slope K^e of the flow stress vs. $d_f^{-1/2}$ curves are a function of strain. σ_0^e and K^e at different strains were obtained from regression calculations of the data and are shown as a function of strain in Fig. 4. It is seen that for three dual-phase steels with approximately constant f_m, both σ_0^e and K^e increase with

Table 1
Quantitative metallographic data and tensile data

Specimen	f_m (%)	d_f (μm)	d_m (μm)	ε_u	$\sigma_{0.2}$ (MPa)	σ_u (MPa)
A1	26.4	36.3	18.3	0.106	341.1	758.1
A2	24.5	21.9	11.0	0.105	340.4	785.6
A3	25.0	18.0	9.9	0.110	355.1	812.5
A4	24.6	12.3	9.4	0.118	355.9	839.5
A5	25.8	8.4	6.7	0.119	368.8	884.1
A6	25.1	5.6	5.0	0.125	394.7	951.5
B1	34.0	34.7	20.9	0.094	369.4	818.0
B2	35.6	20.1	14.4	0.098	388.9	884.5
B3	34.0	17.2	13.1	0.093	385.9	886.7
B4	35.5	13.0	10.2	0.103	398.1	930.2
B5	35.8	9.8	8.4	0.100	412.7	973.4
B6	36.3	7.7	7.1	0.109	421.3	1012.3
C1	43.6	33.0	21.0	0.085	407.6	888.1
C2	43.1	21.6	15.5	0.082	424.8	929.2
C3	45.9	17.4	12.3	0.090	431.1	960.5
C4	44.0	12.9	11.2	0.092	444.9	996.6
C5	45.5	10.6	9.3	0.090	459.8	1064.3
C6	46.0	8.6	8.4	0.094	469.8	1089.7

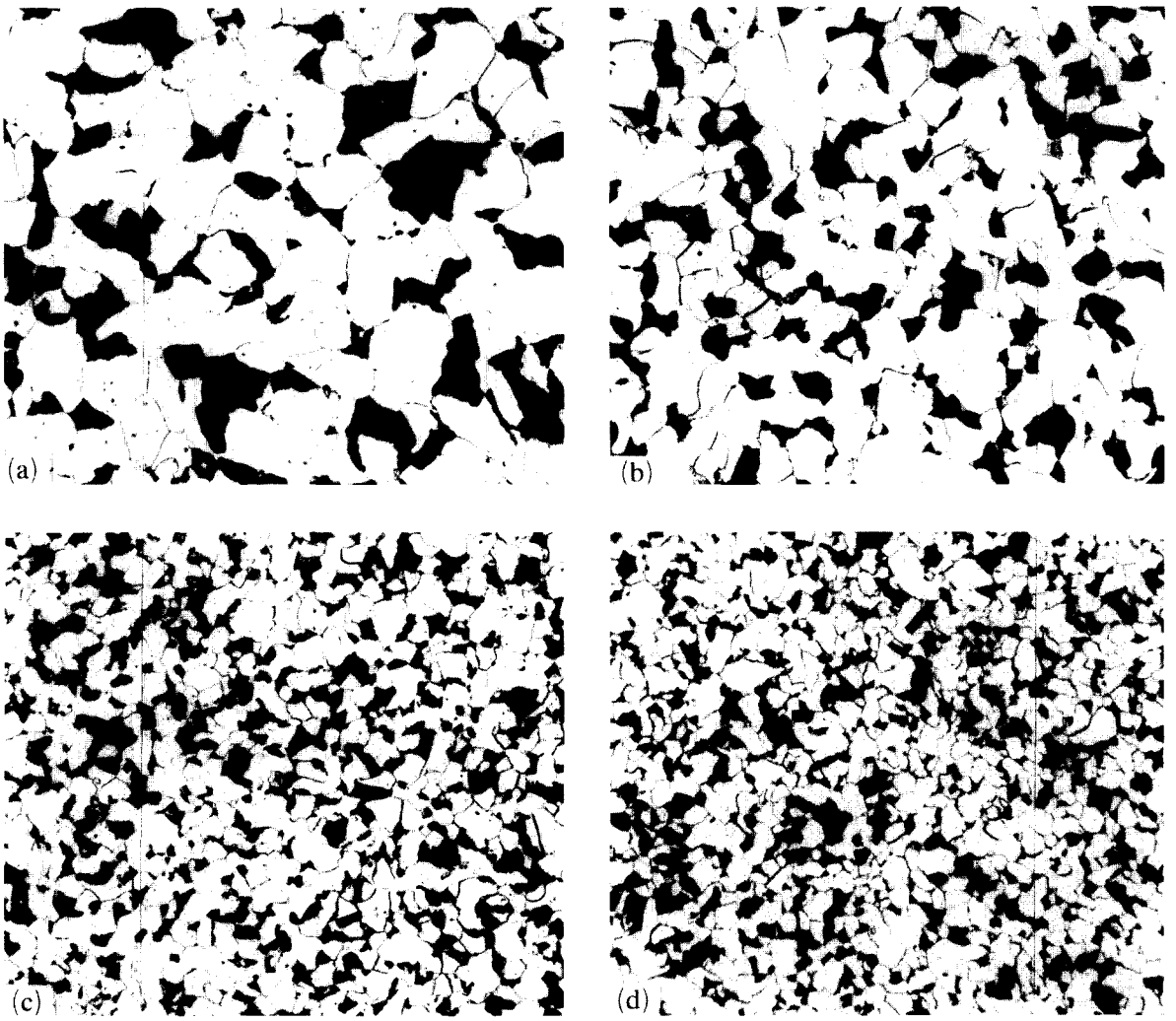

Fig. 1. Optical microstructures of the dual-phase steel: (a) A1, (b) A2, (c) A5, (d) A6; 250×.

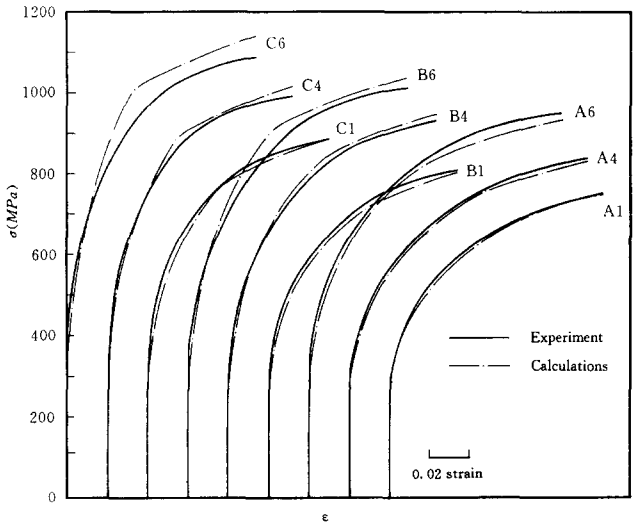

Fig. 2. Experimental and calculated true stress–strain curves of the dual-phase steel.

increasing strain and at high strains K^e remains approximately constant. Both σ_0^e and K^e increase with increasing f_m and the effect of f_m is stronger on K^e than on σ_0^e.

The strain hardening behaviour of this dual-phase steel was analysed using the modified Crussard–Jaoul (C–J) analysis [25] which has been suggested to be more suitable for analysing the strain hardening behaviour of dual-phase steels [26, 27]. The modified C–J analysis is based on the Swift equation [28]

$$\varepsilon = \varepsilon_0 + k\sigma^m \quad (1)$$

where ε and σ are the true strain and true stress, ε_0 and k are constants, and m is the strain hardening exponent. The logarithmic form of Eq. (1), differentiated with respect to strain, is

$$\ln(d\sigma/d\varepsilon) = (1-m)\ln\sigma - \ln(km) \quad (2)$$

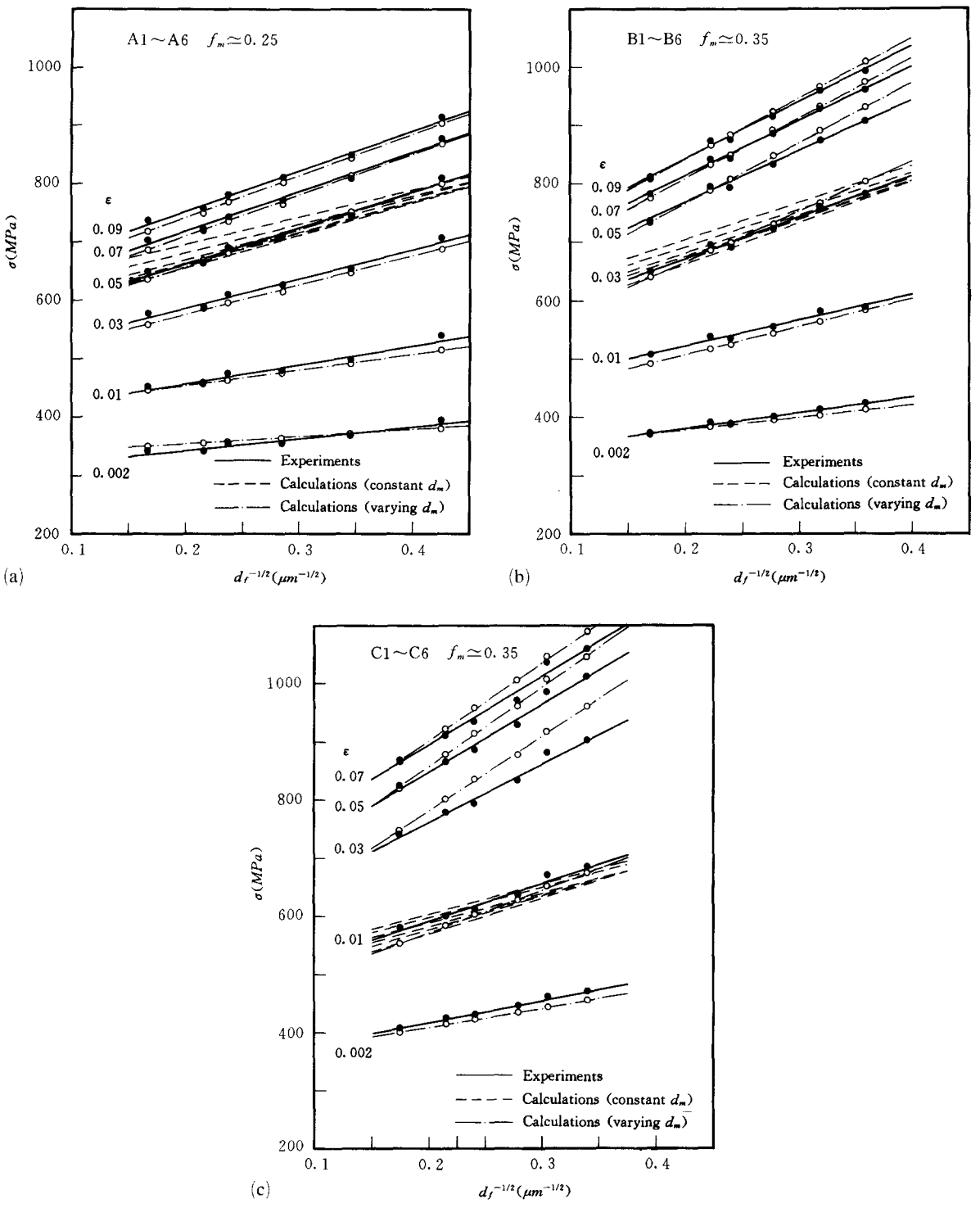

Fig. 3. Experimental and calculated relationship between the flow stress and the inverse square root of ferrite grain size $d_f^{-1/2}$ of the dual-phase steel: (a) A1–A6, $f_m \approx 0.25$; (b) B1–B6, $f_m \approx 0.35$; (c) C1–C6, $f_m \approx 0.45$.

Fig. 5 shows representative $\ln(d\sigma/d\varepsilon)$ vs. $\ln \sigma$ curves of this dual-phase steel. It is seen that the dual-phase steel deforms in two distinct stages. The slopes $(1-m)$ of the $\ln(d\sigma/d\varepsilon)$ vs. $\ln \sigma$ curves in the first (low strain) stage are larger than those in the second (high strain) stage. This two-stage strain hardening behaviour of dual-phase steel has been reported by several authors [26, 27, 29–31]. The transition strains ε_t separating the two stages were measured and are shown in Fig. 6 as a function of f_m. It has been suggested [11, 26, 27, 31] that the two-stage deformation behaviour of dual-phase steels revealed by the modified C–J analysis is

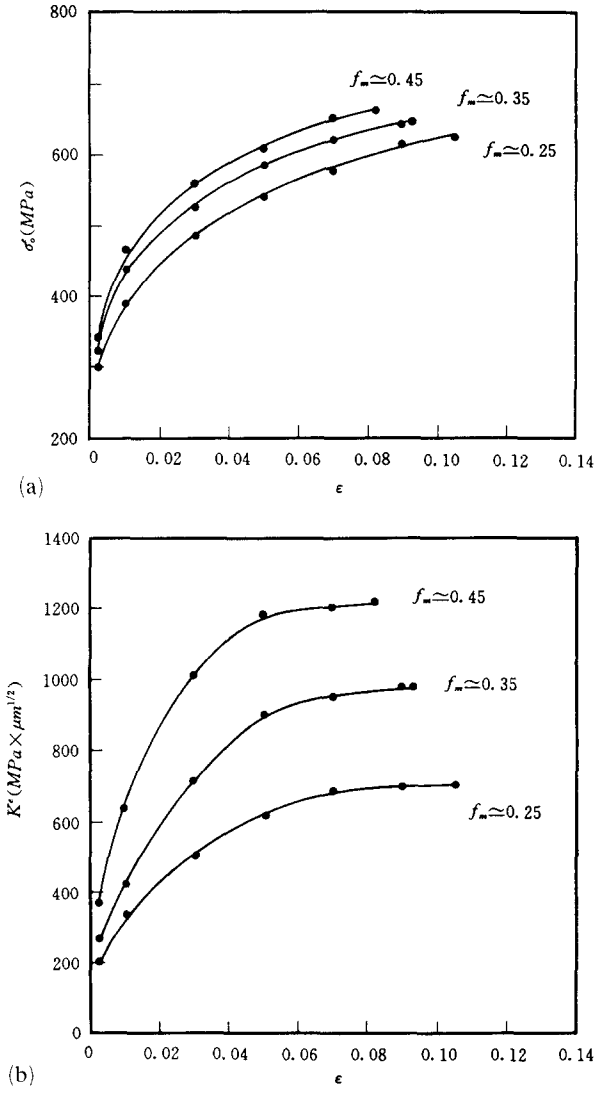

Fig. 4. (a) Dependence of the Hall–Petch intersection σ_0^c on strain in the dual-phase steel; (b) dependence of the Hall–Petch slope K^c on strain in the dual-phase steel.

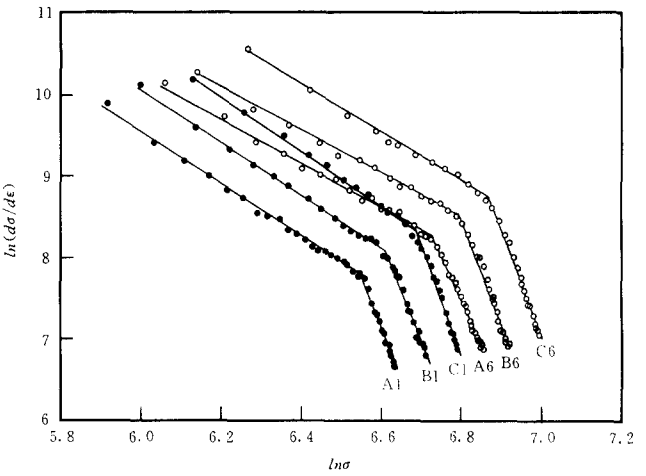

Fig. 5. Representative experimental $\ln(d\sigma/d\varepsilon)$ vs. $\ln\sigma$ curves of the dual-phase steel.

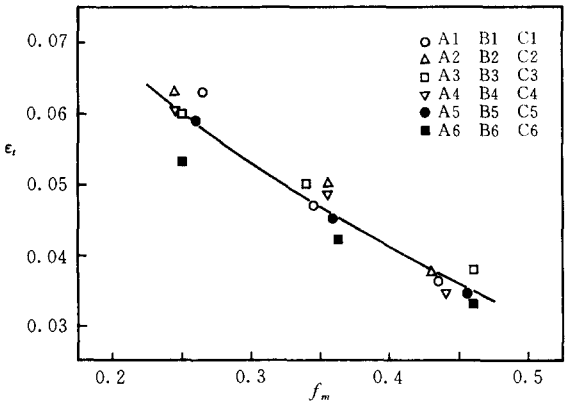

Fig. 6. Dependence of the experimental and calculated transition strain on the volume fraction of martensite in the dual-phase steel.

related primarily to the deformation state of martensite (elastic or plastic) and the development of dislocation structures in the ferrite matrix. In the first low-strain stage, only ferrite deforms plasticly, while martensite remains elastic; in the second high-strain stage, both ferrite and martensite deform plasticly. Therefore, within a certain strain interval around the transition strain ε_t, the deformation state of martensite changes from elastic to plastic.

The strain hardening rates at different strains as a function of ferrite grain size are shown in Fig. 7(a)–(c) for three dual-phase steels having about the same value of f_m. As these figures show, the strengthening effect of grain size mainly occurs at low strains. At low strains the strain hardening rate increases with decreasing grain size, while at high strains the strain hardening rate becomes nearly independent of grain size. At low strains the strain hardening rate of the specimens with larger f_m is markedly higher than that with smaller f_m; at high strains, for example at 0.07 strain, the strain hardening rate of the specimens with larger f_m is slightly lower than that of specimens with smaller f_m.

4. Discussion

4.1. The dependence of flow stress on microstructural variables

Recently, a theoretical model for the relationship between the flow stress and microstructural variables (d_m, d_f and f_m) of dual-phase steel was proposed by Jiang et al. [23] based on the Ashby strain hardening theory [15, 16] and the dislocation pile-up concept.

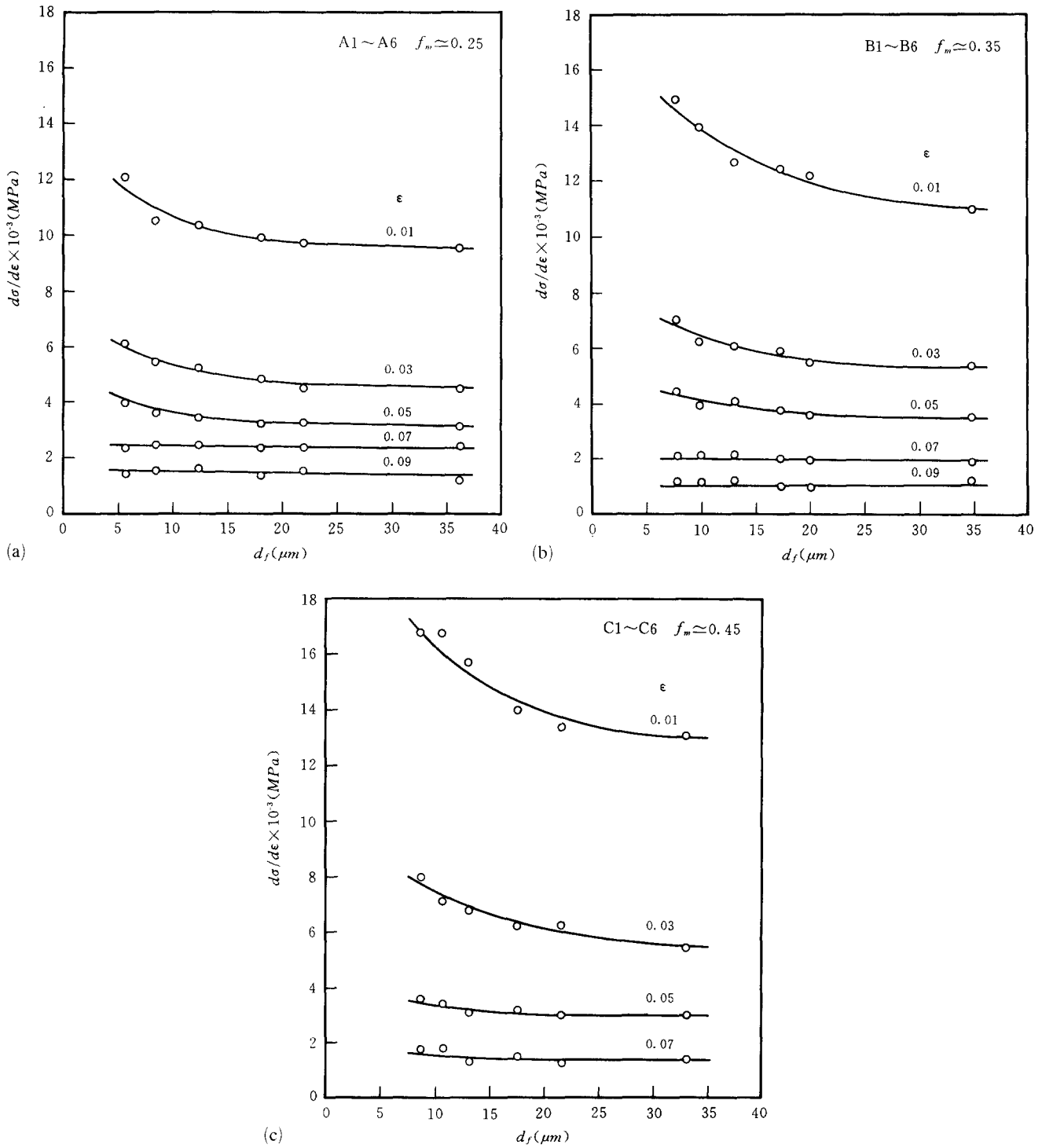

Fig. 7. Change in strain hardening rate with the ferrite grain size of the dual-phase steel: (a) A1-A6, $f_m \approx 0.25$, (b) B1-B6, $f_m \approx 0.35$, (c) C1-C6, $f_m \approx 0.45$.

This model takes into account the inhomogeneous distribution of stress in the ferrite matrix in terms of dislocation density, and divides the ferrite matrix into two regions: the ferrite-martensite phase boundary region with average dislocation density $\rho^s + \rho_m^g$, and the ferrite-ferrite grain boundary region with average dislocation density $\rho^s + \rho_f^g$, where ρ^s is the density of statistically stored dislocations (SSDs) and ρ_m^g and ρ_f^g are the densities of geometrically necessary dislocations (GNDs) [15, 16] in the ferrite-martensite phase boundary region and in the ferrite-ferrite grain boundary region respectively. Based on this model an expres-

sion for the flow stress σ was derived

$$\sigma = \sigma_0 + A[(\rho^s + \rho_f^g)^{1/2}(1-f_m) + (\rho^s + \rho_m^g)^{1/2} f_m] + D(\rho^s + \rho_m^g)^{1/2} f_m (d_m/d_f)^{1/2} \quad (3)$$

where σ_0 is the friction stress of the ferrite matrix, A and D are constants. Substituting the expressions $\rho^s = k\varepsilon_f^n$ [23], $\rho_f^g = \varepsilon_f/(4bd_f)$ and $\rho_m^g = 8Mf_m\varepsilon_f/(bd_m)$ [15, 16] into Eq. (3), the relationship between the flow stress and microstructural variables can be written as

$$\sigma = \sigma_0 + A[(k\varepsilon_f^n + B\varepsilon_f/d_f)^{1/2}(1-f_m) + (k\varepsilon_f^n + Cf_m\varepsilon_f/d_m)^{1/2} f_m] + D(k\varepsilon_f^n + Cf_m\varepsilon_f/d_m)^{1/2} f_m (d_m/d_f)^{1/2} \quad (4)$$

where $A = M^2\alpha Gb/[\sqrt{2} + \ln(\sqrt{2}+1)]$, $B = 1/(4b)$, $C = 8M/b$, and $D = 2\sqrt{2}M^2\alpha Gb/[\sqrt{2}\ln(\sqrt{2}+1)]^2$, k, n and α are material constants, M, G and b are the Taylor factor, the shear modulus and the Burgers vector respectively, and ε_f is the average plastic strain in the ferrite matrix.

It should be noted that the present model is compatible with other deformation theories of two-phase alloys, such as the continuum mechanics models [12, 13] and the dispersion hardening theories [17]. From these theories it can be deduced that the flow stress of a two-phase material can be generally expressed in the following form

$$\sigma = \sigma_A + \sigma_B \quad (5)$$

where σ_A represents the average stress in the soft phase and σ_B is the back stress which is associated with the incompatibility of deformation between the soft phase and the hard phase. It is easy to see that Eq. (3) or Eq. (4) corresponds in form to Eq. (5). The first two terms, which correspond to σ_A, represent the average stress of the ferrite matrix, which includes the contributions of matrix hardening due to ρ^s and the additional grain boundary hardening due to ρ_f^g and phase boundary hardening due to ρ_m^g. The last term, which corresponds to σ_B, represents the back stress which results from the long-range internal stress of the piled-up dislocations due to the inhomogeneous distribution of dislocations in the ferrite matrix. It is evident that there are some differences in form between the present expression for the back stress σ_B and those derived according to the other theories [12, 13, 17]. It is noted, however, that the present expression and the previous expressions for σ_B predict the same tendency of σ_B to vary with the volume fraction of the stronger phase.

4.2. Deformation behaviour of the martensite phase

It is understood that the deformation behaviour of martensite in dual-phase steel depends on its strength, distribution and shape. However, the internal back stress produced by the difference in deformation or strain between two phases also affects the deformation behaviour of martensite and results in load transfer from the ferrite matrix to the martensite phase. So, it would be expected that the behaviour of martensite in a dual-phase steel would be related to the behaviour of ferrite. In the following, an attempt is made to derive an expression for the stress of martensite based on the model of Jiang et al. [23]. This model shows that the dislocation pile-up due to plastic shear in the ferrite matrix would produce stress fields in the adjacent martensite particles which would result in the shear deformation of martensites. By using two derived relations (Eqs. (9) and (10)) in ref. [23], a relationship between the average shear stress in martensite τ_m' due to the stress field of the pile-up and the shear stress in the ferrite matrix adjacent to the martensite τ_f can be obtained

$$\frac{\sqrt{2}}{2}\left(\frac{d_m}{d_f}\right)^{1/2}\tau_m' = \left\{\frac{1}{\sqrt{2}+\ln(\sqrt{2}+1)} + \frac{2\sqrt{2}}{[\sqrt{2}+\ln(\sqrt{2}+1)]^2} \times \left(\frac{d_m}{d_f}\right)^{1/2}\right\}\tau_f \quad (6)$$

where the directions of the shear stresses τ_m' and τ_f are dependent of the orientations of the existing slip planes in two adjacent ferrite and martensite grains. The shear stresses τ_m' and τ_f can be converted further into the normal stresses σ_m' and σ_f using the Taylor factor $M(\sigma = M\tau)$. In this case, σ_m' and σ_f have the same direction as the tensile direction and the stress σ_f can be written as $\sigma_f = M\alpha Gb(\rho^s + \rho_m^g)^{1/2}$ [23]. However, because martensite is a discontinuous phase, the effect of the end loading stress in the tensile direction should be considered. So, in adition to σ_m', the stress carried by martensite should include an additional contribution from the end loading stress. As an approximate treatment, the end loading stress should be equal to the average flow strength of the ferrite matrix near the martensite, i.e. $\sigma_0 + M\alpha Gb(\rho^s + \rho_m^g)^{1/2}$. Thus, the stress of the martensite phase σ_m can be expressed as

$$\sigma_m = \sigma_0 + [E' + F'(d_f/d_m)^{1/2}](\rho^s + \rho_m^g)^{1/2} \quad (7)$$

where E' and F' are constants. Further, σ_m can be expressed in the following form using the expressions for ρ^s and ρ_m^g

$$\sigma_m = \sigma_0 + [E + F(d_f/d_m)^{1/2}](k\varepsilon_f^n + Cf_m\varepsilon_f/d_m)^{1/2} \quad (8)$$

where $E = M\alpha Gb\{1 + 4/[\sqrt{2} + \ln(\sqrt{2}+1)]^2\}$ and $F = M\alpha Gb\{\sqrt{2}/[\sqrt{2} + \ln(\sqrt{2}+1)]\}$. Eqs. (7) and (8) show that the stress of the martensite phase is related to the strain hardening of the ferrite matrix $(\rho^s + \rho_m^g)$ and can

be expressed as a function of microstructural variables (d_m, d_f and f_m) and strains (ε_f). These two equations describe the form of the load transfer from ferrite to martensite.

According to Eqs. (7) and (8), the stress carried by martensite σ_m increases with the strain hardening of ferrite ($\rho^s + \rho^g_m$), when σ_m increases up to a level equal to the yield strength of martensite, the martensite starts deforming plasticly, the deformation state of martensite transforms from elastic to plastic. It is possible to determine the onset of plastic deformation of martensite (transition strain) using Eq. (8), provided that one knows the yield strength of martensite and relative material constants and microstructural variables. Since data for the yield strength of martensite are lacking, a quantitative calculation of the transition strain cannot be given in the present case. However, the observed variation in the transition strain (ε_t) with the microstructural variables (Fig. 6) by the modified C–J analysis can be interpreted generally using Eq. (8).

It is apparent from Eq. (8) that the transition strain ε_t depends on the yield strength of martensite: the higher the yield strength, the larger the transition strain ε_t. If the yield strength of martensite is very high, ε_t may be even larger than the maximum uniform true strain ε_u, which means that martensite would remain elastic over the uniform plastic strain range. However, increasing the strain hardening in the ferrite matrix would force the martensite to deform plasticly earlier. Therefore, the observed decrease in ε_t with increasing f_m is attributed to increased strain hardening in the ferrite matrix ρ^g_m and the decrease in the yield strength of martensite with increasing f_m. Because the effects of d_m and d_f on ε_t are reverse, as indicated in Eq. (8), and the yield strength of martensite may be related to d_m, the individual effects of d_m and d_f on ε_t cannot be distinguished in this figure. However, it can still be seen that the specimens with smaller grain sizes tend to have smaller ε_t.

4.3. Flow stress and strain hardening rate

When the bulk strain ε is larger than the transition strain ε_t, because of the plastic deformation of martensite, the requirement of compatibility of deformation between two phases no longer increases. According to Ashby's analysis [15, 16] this will result in a decrease in the stored rate of GNDs ρ^g_m. In this case, the linear variation of ρ^g_m with strain will no longer be valid. Speich and Miller [7] have shown that at higher strains the density of GNDs ρ^g_m would remain constant so that the strain hardening of dual-phase steel is due mainly to the increase in the density of SSDs ρ^s. In addition, the dynamic recovery processes of dislocation structures at higher strains [32] would also lower the stored rate of GNDs ρ^g_m. Therefore, it can be assumed roughly that after ε_t, ρ^g_m remains constant. In order to calculate the true stress–strain curves of this dual-phase steel using Eq. (3), the constants k, n and α were chosen to be 6×10^{10} cm^{-2}, 0.85 and 0.5 respectively from the analysis [23]. The other material constants were chosen as $M=2.733$, $G=8.07\times10^4$ MPa and $b=2.48\times10^{-8}$ cm [19, 23]. σ_0 is taken as 260 MPa from the experimental true stress–strain curves of this dual-phase steel. After the plastic deformation of martensite, the plastic strain in martensite ε_m will contribute to the bulk strain ε. It has been observed experimentally [10, 33] that the plastic strain of martensite ε_m increases linearly with the bulk strain ε and the slopes of the experimental ε_m vs. ε curves are less affected by grain sizes, volume fraction, carbon content and heat treatment conditions and vary within a very small range (about 0.25–0.3 [10], 0.2–0.4 [33]). According to these studies, when $\varepsilon \geqslant \varepsilon_t$, ε_m may be written approximately as $\varepsilon_m = 0.3(\varepsilon_m - \varepsilon_t)$. From the relation $\varepsilon = \varepsilon_f(1-f_m) + \varepsilon_m f_m$, one can obtain $\varepsilon_f = [\varepsilon - 0.3(\varepsilon - \varepsilon_t)f_m]/(1-f_m)$. When $\varepsilon \leqslant \varepsilon_t$, one has $\varepsilon_f = \varepsilon/(1-f_m)$. Substituting these two relations into Eq. (3) and using the assumption on ρ^g_m that when $\varepsilon \geqslant \varepsilon_t$, $\rho^g_m = 8Mf_m\varepsilon_t/[(1-f_m)bd_m]$, and the relative data, the true stress–strain curves can be calculated; the results are shown in Fig. 2. It can be seen that good agreement is obtained.

The calculations show that the average flow stresses of ferrite σ_A (the first two terms on the right-hand side of Eq. (3)) increase little with increasing f_m and decreasing grain size. The major strengthening effects of f_m and grain size on the flow stress σ result from the back stress σ_B (the last term on the right of Eq. (3)). The calculated σ_B as a function of strain ε is shown in Fig. 8. As shown, at low strains ($\varepsilon \leqslant \varepsilon_t$) σ_B rises rapidly with increasing ε, and at high strains ($\varepsilon \geqslant \varepsilon_t$) the increase in σ_B becomes markedly slow. At given ε, σ_B increases markedly with increasing f_m and decreasing grain size. These predicted variations in σ_B with ε, f_m and grain size are found to be well consistent with recent experimental results of Bauschinger effect testing of dual-phase steel [34].

The variation of the strain hardening rate in Fig. 7 can be explained using Eqs. (3) or (4). Since ρ^s is independent of the grain size, ρ^g_f is very small in comparison with ρ^s or ρ^g_m and the ratio $(d_m/d_f)^{1/2}$ in Eq. (3) varies within a very small range (see Table 1), the apparent difference in strain hardening rate between specimens with different grain sizes is attributed to the difference in ρ^g_m. At low strains, where ρ^g_m increases rapidly (linearly) with ε, ρ^g_m can provide a larger stress increment. So, the strain hardening rate in specimens with smaller grain sizes is higher than that in specimens with larger grain sizes. At high strains, because ρ^g_m

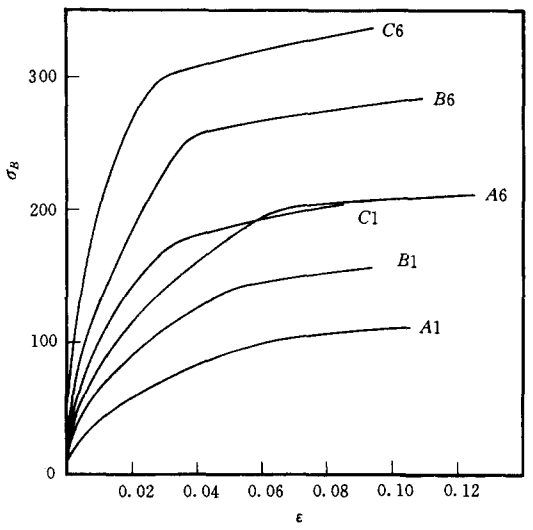

Fig. 8. Representative back stress vs. strain curves calculated using Eq. (4).

remains constant it cannot provide any stress increment, and the increase in stress results from the increase in ρ^s. Therefore, the strain hardening rate becomes independent of grain size. As indicated in Eq. (3), as f_m increases the contributions of both ρ^s and ρ^g_m to the flow stress increase. However, increasing f_m also forces martensite to deform plasticly at lower strain (ε_t becomes small (Fig. 6)). So, over the whole strain range, the average decreasing rate of strain hardening in the specmens with larger f_m is larger than that in specimens with smaller f_m. Such strain hardening behaviour would result in a higher strength but lower ductility [31].

4.4. The Hall–Petch relation

If the contribution of ρ^g_f, which is very small in comparison with ρ^s or ρ^g_m, is neglected, and using the assumption on ρ^g_m, Eq. (3) can be written as

$$\sigma = \sigma_0^c + K^c d_f^{-1/2} \tag{9}$$

where

$$\sigma_0^c = \sigma_0 + A[(k\varepsilon_f^n)^{1/2}(1-f_m) + (k\varepsilon_f^n + Cf_m\varepsilon_f^c/d_m)^{1/2} f_m]$$

$$K^c = D(k\varepsilon_f^n + Cf_m\varepsilon_f^c/d_m)^{1/2} f_m d_m^{1/2}$$

Where when $\varepsilon \leqslant \varepsilon_t$, $\varepsilon_f^c = \varepsilon_f$; when $\varepsilon \geqslant \varepsilon_t$, $\varepsilon_f^c = \varepsilon_t/(1-f_m)$. This equation shows that the dependence of the flow stress of dual-phase steel on the ferrite grain size follows the Hall–Petch relation, where the Hall–Petch parameters σ_0^c and K^c are functions of ε (or ε_f), f_m and d_m. According to the preceding analysis, the parameter σ_0^c corresponds to the average flow stress of the ferrite matrix σ_A, and the parameter K^c is related to the back stress σ_B.

Eq. (9) predicts that at given ε and f_m, if d_m is constant when d_f varies, a linear relation between the flow stress and $d_f^{-1/2}$ can be obtained. However, for dual-phase steels, it is generally difficult to keep d_m constant while only changing d_f. Therefore, for most dual-phase steels, a precise linear relationship between the flow stress and $d_f^{-1/2}$ may not be maintained. Nevertheless, if d_m varies in the same manner as d_f, an approximate linear relationship between the flow stress and $d_f^{-1/2}$ can still be observed.

The calculated σ vs. $d_f^{-1/2}$ relations of the dual-phase steel using Eq. (9) are shown in Fig. 3. In the calculations, f_m and ε_t are taken as the average values of all specimens with approximately constant f_m. The agreements between the calculations and experiments were good. The calculated σ_0^c and K^c with constant d_m at a selected strain (the dashed lines, Fig. 3) are different from those calculated with d_m varying as d_f (the solid lines); however, in the present case the difference is very small. This indicates that the Hall–Petch parameters in dual-phase steel are related to the relationship between d_m and d_f.

Eq. (9) shows that σ_0^c depends on ρ^s and ρ^g_m; as f_m increases the contribution of ρ^g_m increases while that of ρ^s is less affected. This was supported by experimental results (Fig. 4(a)). It can be seen that at given strains the increase in σ_0^c is small as f_m increases. This means that the Hall–Petch intersection σ_0^c of dual-phase steel is mainly controlled by the density of SSDs ρ^s, while the contribution of the density of GNDs ρ^g_m is relatively small, especially when f_m is small. K^c depends on ρ^s and ρ^g_m, and f_m has a stronger influence on K^c than on σ_0^c. Therefore, the marked increase in K^c with increasing f_m (Fig. 4(b)) is due to the fact that the contributions of ρ^s and ρ^g_m increase with f_m. It can be seen from Fig. 4(b) that at high strains K^c remains approximately constant. This indicates that at high strains the strengthening effect of grain size diminishes. It can be noted that the strain point after which K^c remains constant corresponds approximately to the average values of the transition strain ε_t (Fig. 6). This indicates that the Hall–Petch slope of dual-phase steel is dependent on the plastic deformation of martensite (or the yield strength of martensite), the strengthening effect of grain size for dual-phase steel would be lowered by the plastic deformation of martensite.

5. Conclusions

(1) An expression for the stress of martensite in dual-phase steel was proposed based on the theoretical model (ref. [23]), which can be written as

$$\sigma_m = \sigma_0 + A[E' + F'(d_f/d_m)^{1/2}](\rho^s + \rho^g_m)^{1/2}$$

which shows that the stress of martensite is related to strain hardening in the ferrite matrix ($\rho^s + \rho_m^g$).

(2) The onset of plastic deformation of martensite (the transition strain) in dual-phase steel shifts to a lower strain as f_m increases and as the yield strength of martensite decreases. The observed transition strain ε_t in the $\ln(d\sigma/d\varepsilon)$ vs. $\ln\sigma$ curves was well interpreted by the proposed expression.

(3) Decreasng the grain size and increasing f_m increase the flow stress and raise the strain hardening rate at low strains, but hardly affect the strain hardening rate at high strains, which can be explained by the present theoretical analysis.

(4) The dependence of flow stress of this dual-phase steel on the ferrite grain size obeys the Hall–Petch relation, i.e. $\sigma = \sigma_0^e + K^e d_f^{-1/2}$. The Hall–Petch intersection σ_0^e and slope K^e are functions of ε, f_m and d_m. f_m has a much stronger influence on K^e than on σ_0^e. The observed Hall–Petch behaviour can be well described by the model developed previously by Jiang et al. [23].

References

[1] S. T. Mileiko, *J. Mater. Sci., 4* (1969) 974.
[2] R. G. Davies, *Metall. Trans. A, 9* (1978) 41.
[3] R. G. Davies, *Metall. Trans. A, 9* (1978) 671.
[4] G. Thomas and J. Y. Koo, in R. A. Kot and J. W. Morris (eds.), *Structure and Properties of Dual Phase Steels*, Metallurgical Society of AIME, New York, 1979, p. 183.
[5] I. Tamura, Y. Tomota and H. Ozawa, *Proc. 3rd Int. Conf. on the Strength of Metals and Alloys, Inst. of Metals and Iron and Steel Inst., Cambridge, London, 1973*, Vol. 1, p. 611.
[6] H. Fischmeister and B. Karlsson, *Z. Metallkd., 68* (1977) 311.
[7] G. R. Speich and R. L. Miller, in R. A. Kot and J. W. Morris (eds.), *Structure and Properties of Dual Phase Steels*, Metallurgical Society of AIME, New York, 1979, p. 145.
[8] N. C. Goel, S. Sangal and K. Tangri, *Metall. Trans. A, 16* (1985) 2013.
[9] S. Sangal, N. C. Goel and K. Tangri, *Metall. Trans. A, 16* (1985) 2023.
[10] Y. L. Su and J. Gurland, *Mater. Sci. Eng., 95* (1987) 151.
[11] J. Lian, Z. Jiang and J. Liu, *Mater. Sci. Eng. A, 147* (1991) 55.
[12] Y. Tomota, K. Kuroki, T. Mori and I. Tamura, *Mater. Sci. Eng., 24* (1976) 85.
[13] C. Kim, *Metall. Trans. A, 19* (1988) 1263.
[14] M. F. Ashby, *Philos. Mag., 14* (1966) 1157.
[15] M. F. Ashby, *Philos. Mag., 21* (1970) 399.
[16] M. F. Ashby, in A. Kelly and R. B. Nicholson (eds.), *Strengthening Methods in Crystals*, Elsevier, Amsterdam, 1971, p. 137.
[17] L. M. Brown and W. A. Stobbs, *Philos. Mag., 23* (1971) 1185, 1201.
[18] N. K. Ballinger and T. Gladman, *Met. Sci., 15* (1981) 95.
[19] C. A. N. Lanzillotto and F. B. Pickering, *Met. Sci., 16* (1982) 371.
[20] D. A. Burford, D. K. Matlock and G. Krauss, in H. J. McQueen, J. P. Bailon, J. I. Dickson, J. J. Jonas and M. G. Akben (eds.), *Strength of Metals and Alloys*, Oxford, 1985, Vol. 1, p. 189.
[21] A. M. Sarosiek and W. S. Owen, *Scr. Metall., 17* (1983) 227.
[22] J. Gerbase, J. D. Embury and R. M. Hobbs, in R. A. Kot and J. W. Morris (eds.), *Structure and Properties of Dual Phase Steels*, Metallurgical Society of AIME, New York, 1979, p. 118.
[23] Z. Jiang, J. Liu and J. Lian, *Acta Metall. Mater., 40* (1992) 1587.
[24] T. Tanaka, M. Nishida, K. Hashiguchi and T. Kato, in R. A. Kot and J. W. Morris (eds.), *Structure and Properties of Dual Phase Steels*, Metallurgical Society of AIME, New York, 1979, p. 221.
[25] R. E. Reed-Hill, W. R. Cribb and S. N. Monteiro, *Metall. Trans. A, 4* (1973) 2665.
[26] W. R. Cribb and J. M. Rigabee, in R. A. Kot and J. W. Morris (eds.), *Structure and Properties of Dual Phase Steels*, Metallurgical Society of AIME, New York, 1979, p. 91.
[27] Y. Tomita and K. Okabagashi, *Metall. Trans. A, 16* (1985) 865.
[28] H. W. Swift, *J. Mech. Phys. Solids, 1* (1952) 1.
[29] L. F. Ramos, D. K. Matlock and G. Krauss, *Metall. Trans. A, 10* (1979) 259.
[30] F. H. Samuel, *Mater. Sci. Eng., 92* (1987) L1.
[31] Z. Jiang, J. Lian and J. Chen, *Mater. Sci. Technol., 8* (1992) 1075.
[32] D. A. Korzekwa, D. K. Matlock and G. Krauss, *Metall. Trans. A, 10* (1984) 1221.
[33] H. P. Shen and T. C. Lei, *Met. Sci., 18* (1984) 297.
[34] L. Zhonghua and G. Haicheng, *Metall. Trans. A, 21* (1990) 717, 725.